

Synthesis of a Dinuclear Ruthenabicyclic Complex and Its Ligand-Substitution Reactions

Yoshihiko Yamamoto,^{*,[a]} Yumiko Miyabe,^[b] and Kenji Itoh^[b]

Keywords: Alkyne ligands / Carbonyl ligands / Metallacycles / Phosphane ligands / Ruthenium

A trinuclear carbonylruthenium complex, $[\text{Ru}_3(\text{CO})_{12}]$, was treated with diynes bearing ester, phenyl, or trimethylsilyl groups on the alkyne termini to give rise to various complexes. A diyne diester afforded a dinuclear ruthenacycle complex similar to known iron ferrole complexes and a mononuclear ruthenacyclopentadiene complex. The selectivity for the formation of these products varied depending on the ratio of the diyne diester toward $[\text{Ru}_3(\text{CO})_{12}]$. When a phenyl-substituted diyne was employed, a cyclopentadienone complex was formed together with the expected dinuclear ruthenacycle complex. In contrast, a bis(trimethylsilyl)diyne gave the corresponding cyclopentadienone complex as the only product. Treatment of the obtained ruthenabicyclic complex with trimethylamine oxide (Me_3NO) gave a mono(trimethylamine) complex, which was further converted into various phosphane complexes upon reaction with phosphanes in refluxing THF. The corresponding monophosphane complexes

were obtained for all monodentate or bidentate phosphanes except for bis(diphenylphosphanyl)methane, which afforded a bridging bis(phosphane) complex. In contrast, when an isolated monodentate phosphane complex of 1,2-bis(diphenylphosphanyl)ethane and diphenyl(2-pyridyl)phosphane was treated with Me_3NO , P-P or P-N chelate complexes were formed, respectively. The dinuclear mono(amine)ruthenacycle complex also reacted with dimethyl butynedioate (dimethyl acetylenedicarboxylate, DMAD) in refluxing THF to afford a novel $\mu\text{-}\eta^2$ -alkyne complex together with the [2+2+2] cycloadduct between the diyne and DMAD. The highly electron-deficient character of DMAD is imperative for the formation of the μ -alkyne complex. Methyl propiolate and diphenylacetylene gave no corresponding μ -alkyne complexes.

(© Wiley-VCH Verlag GmbH & Co. KGaA, 69451 Weinheim, Germany, 2004)

Introduction

Metallacyclopentadienes have received considerable attention because of their close relevance to alkyne cyclooligomerization reactions.^[1] The oxidative cyclization of two alkyne molecules with a low-valent transition-metal fragment gives rise to a metallacyclopentadiene. The diene moiety of a metallacyclopentadiene can be coordinated by another metal fragment to form a dinuclear complex.^[2] Among such dinuclear metallacycle complexes, iron ferrole complexes, $[\text{Fe}_2(\text{CO})_6(\text{RC}_2\text{R}')_2]$,^[3,4] and their cobalt analogues^[5] have been extensively explored as intermediates for the formation of a variety of organic molecules from alkynes and carbonyl transition-metal complexes. With respect to the ruthenium analogues, most examples have been obtained from the reaction of a trinuclear carbonyl cluster, $[\text{Ru}_3(\text{CO})_{12}]$ (**1**), with monoalkynes and conjugated polyalkynes.^[6,7] However, the reported yields of the dinuclear complexes were not high

and generally below 50%. Therefore, further exploration of the dinuclear ruthenacycle complexes awaits an improved synthetic method.

We have recently developed ruthenium-catalyzed [2+2+2] cycloadditions of 1,6-diynes with unsaturated molecules, resulting in the formation of benzenes, cyclohexadienes, pyridines, pyridones, etc.^[8] These cycloadditions essentially did not take place with monoalkynes, except for electron-deficient ones, indicating that the 1,6-diyne substrates play a critical role in the formation of the ruthenacycle key intermediate: the oxidative cyclization of the 1,6-diynes is entropically more favorable than that of monoalkynes. With these facts in mind, we further investigated the reaction of **1** with diynes to establish a highly efficient route to bicyclic analogues of the dinuclear ruthenacycle complexes.^[9] Herein we report on the efficient synthesis of a dinuclear ruthenabicyclic complex, using a diyne diester as an alkyne substrate, and its ligand-substitution reactions.

Results and Discussion

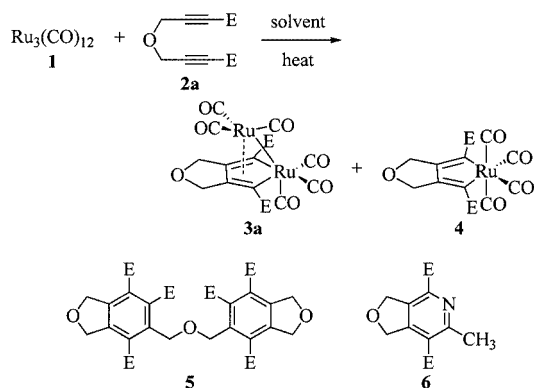
Reaction of $[\text{Ru}_3(\text{CO})_{12}]$ with Diynes

At the outset, the diyne diester **2a** bearing methoxycarbonyl terminal substituents was examined as a diyne sub-

^[a] Department of Applied Chemistry, Graduate School of Engineering, Nagoya University, Chikusa, Nagoya 464-8603, Japan
Fax: + 81-52-789-3209
E-mail: yamamoto@apchem.nagoya-u.ac.jp

^[b] Department of Molecular Design and Engineering, Graduate School of Engineering, Nagoya University, Chikusa, Nagoya 464-8603, Japan

strate (Scheme 1) because the electron-deficient alkyne termini favor oxidative cyclization with a low-valent transition-metal fragment.^[10] The trinuclear cluster $[\text{Ru}_3(\text{CO})_{12}]$ (**1**) and **2a** were allowed to react under various reaction conditions (Table 1). In toluene, **1** and 2 equiv. of **2a** were heated at 110 °C under Ar for 0.5 h (run 1). The TLC analysis of the crude reaction mixture showed the complete consumption of **2a**. Separation by silica-gel chromatography gave pure **3a**. In the ^1H NMR spectrum of **3a**, the absorptions of the methylene protons adjacent to the ether oxygen atom appear at $\delta = 4.80$ (dd, $J_{\text{H,H}} = 15.3, 2.4$ Hz, 2 H) and 5.08 (dd, $J_{\text{H,H}} = 15.3, 2.4$ Hz, 2 H) ppm, indicative of the diyne having undergone oxidative cyclization. This was also confirmed by the IR spectrum, which shows no alkyne absorption. Instead, strong absorptions corresponding to the CO ligands were observed around 2000 cm^{-1} . The ^{13}C NMR spectrum shows the resonance of the CO ligands at $\delta = 192.21, 193.60,$ and 194.37 ppm as well as three sp^2 - and two sp^3 -carbon signals. Finally, single-crystal X-ray crystallography unambiguously revealed that **3a** is a dinuclear ruthenacycle complex, as shown in Figure 1. The unit cell contains two crystallographically unique molecules **3a(A)** and **3a(B)**. Similar to known ferrole-type complexes,^[6] the $[\text{Ru}_2(\text{CO})_6]$ fragments of **3a** have a “non-sawhorse” geometry typified by a semi-bridging CO ligand and an Ru–Ru single bond of about 2.72 Å, which is within the range of Ru–Ru single bond lengths found previously.^[6] In **3a(A)**, the Ru2–C2 and Ru2–C7 bond lengths are 2.071(9) and 2.105(8) Å, respectively, and the C2–C3 and C6–C7 bonds [1.467(11) and 1.478(10) Å] are longer than the C3–C6 bond [1.351(12) Å]. In contrast, the Ru2–C2 and Ru2–C7 bonds [2.096(7) and 2.114(8) Å] in **3a(B)** are longer than those in **3a(A)**, and the C3–C6 bond of 1.456(11) Å is longer than the C2–C3 and C6–C7 bonds [1.369(12) and 1.375(12) Å] in **3a(B)**. These data indicate that **3a(A)** and **3a(B)** are represented as structures **I** and **II**, respectively, in Scheme 2. These structural features are quite similar to the previously reported tetrakis(methoxycarbonyl) analogue.^[6d]



Scheme 1. Reaction of $[\text{Ru}_3(\text{CO})_{12}]$ (**1**) with diyne diester **2a**

Together with **3a**, the diyne trimer **5** was also obtained in 13% yield as a result of the $[2+2+2]$ cycloaddition of **2a**.^[10c,10d] In addition, 51% of **1** was recovered intact. To

improve the yield of **3a**, the reaction conditions were further optimized. Using acetonitrile instead of toluene as a solvent successfully suppressed the formation of **5**, although a trace amount of pyridine **6** was formed by $[2+2+2]$ cycloaddition of **2a** with CH_3CN (Table 1, run 2). As a consequence, the yield of **3a** was raised to 56%. Although **1** was almost completely consumed, total recovery of ruthenium (**3a** and recovered **1**) was not more than 60%. This was probably because **1** decomposed under argon with concomitant extrusion of CO. Thus, the reaction was then conducted under 1 atm of CO in refluxing CH_3CN (run 3). The starting **2a** was totally consumed within 1 h. However, the yield of **3a** was not improved, and an additional product, **4**, was obtained as well as recovered **1**. The IR spectrum of **4** is very similar to that of **3a**. The absorptions of a conjugated carbonyl group and the CO ligands are observed at 1676 cm^{-1} and around 2000 cm^{-1} , respectively. In contrast to **3a**, only two singlet signals assigned to $-\text{OCH}_2-$ and $-\text{OCH}_3$ with a 2:3 integral ratio appear at $\delta = 4.65$ and 3.75 ppm, respectively, in the ^1H NMR spectrum. Furthermore, in the ^{13}C NMR spectrum, five sp^2 -carbon peaks are observed at $\delta = 171$ –190 and 133.66 ppm along with sp^3 -carbon peaks assigned to $-\text{OCH}_2-$ and $-\text{OCH}_3$ at $\delta = 70.62$ and 51.98 ppm, respectively. These data suggest that **4** is a highly symmetrical carbonylruthenium complex derived from **2a**. The detailed structural assignment was accomplished by X-ray crystallographic analysis. As shown in Figure 1, **4** is a mononuclear ruthenabicyclic complex bearing four CO ligands. The unit cell contains two crystallographically unique molecules. The geometry of the ruthenium center is distorted octahedral with the basal plane consisting of the two CO ligands and the metallacycle carbon atoms C2 and C7; there are two apical CO ligands. The C13–Ru1–C14 angles are $164.5(3)^\circ$ and $165.0(3)^\circ$. The ruthenacycle moieties present normal metallacyclopentadiene geometries with C_α – C_β bond lengths ranging from 1.307(13) to 1.388(12) Å, which are shorter than the C_β – C_β bonds [1.471(12) and 1.432(12) Å]. The Ru– C_α distances, ranging from 2.110(10) to 2.172(8) Å, are similar to those of typical Ru– sp^2 -C single bonds.^[11]

Further optimization of the reaction conditions was carried out by performing the reaction under higher CO pressure in an autoclave. Under 5 atm of CO, **1** and 2 equiv. of **2a** were heated in CH_3CN at 120 °C for 12 h to afford **3a** in an improved isolated yield of 74% together with **4** in 20% yield (Table 1, run 4). Trace amounts of **6** and recovered **1** were also detected. Similar results were obtained from the reaction under 10 atm of CO (run 5). The reduced amounts of the diyne **2a** increased the product selectivity in favor of the dinuclear complex **3a**. The use of 1.5 equiv. of **2a** ($\text{2a}/\text{Ru} = 1:2$) gave predominantly **3a** in 87% yield (run 6). The reaction terminated after 1 h resulted in lower conversion of **1** (70%), and, interestingly, both **3a** and **4** were obtained in 43 and 21% yields, respectively (run 7). This result suggests that the initially formed mononuclear complex **4** might be converted into the dinuclear complex **3a**. In fact, the isolated **4** was treated with **1** (1 equiv. Ru) in CH_3CN at 120 °C under 5 atm of CO for 12 h to afford **3a** in 78% yield together with recovered **4** and **1** (18% and 23%, respec-

Table 1. Reaction of $\text{Ru}_3(\text{CO})_{12}$ (**1**) with diynes **2**

| Run | 2 , R (equiv.) | Conditions | Products (yield [%]) ^[a] | Recovered 1 [%] |
|-----|--|--|---|------------------------|
| 1 | 2a , CO_2CH_3 (2) | Ar, toluene, reflux, 0.5 h | 3a (27), 5 (13) | 51 |
| 2 | 2a , CO_2CH_3 (2) | Ar, CH_3CN , reflux, 0.5 h | 3a (56), 6 (trace) | 4 |
| 3 | 2a , CO_2CH_3 (2) | CO (1 atm), CH_3CN , reflux, 1 h | 3a (60), 4 (9), 6 (trace) | 10 |
| 4 | 2a , CO_2CH_3 (2) | CO (5 atm), CH_3CN , 120 °C, 12 h | 3a (74), 4 (20), 6 (trace) | trace |
| 5 | 2a , CO_2CH_3 (2) | CO (10 atm), CH_3CN , 120 °C, 12 h | 3a (62), 4 (24), 6 (trace) | 9 |
| 6 | 2a , CO_2CH_3 (1.5) | CO (5 atm), CH_3CN , 120 °C, 12 h | 3a (86), 6 (trace) | 9 |
| 7 | 2a , CO_2CH_3 (1.5) | CO (5 atm), CH_3CN , 120 °C, 1 h | 3a (43), 4 (21), 6 (trace) | 30 |
| 8 | 2b , Ph (1.5) | CO (5 atm), CH_3CN , 120 °C, 12 h | 3b (20), 7b (8) | 63 |
| 9 | 2b , Ph (3) | CO (5 atm), CH_3CN , 120 °C, 12 h | 3b (25), 7b (12) | 37 |
| 10 | 2c , $\text{Si}(\text{CH}_3)_3$ (1.5) | CO (5 atm), CH_3CN , 120 °C, 12 h | 7c (41) | 43 |
| 11 | 2c , $\text{Si}(\text{CH}_3)_3$ (3) | CO (5 atm), CH_3CN , 120 °C, 12 h | 7c (76) | 8 |

^[a] Isolated yield based on $\text{Ru}_3(\text{CO})_{12}$.

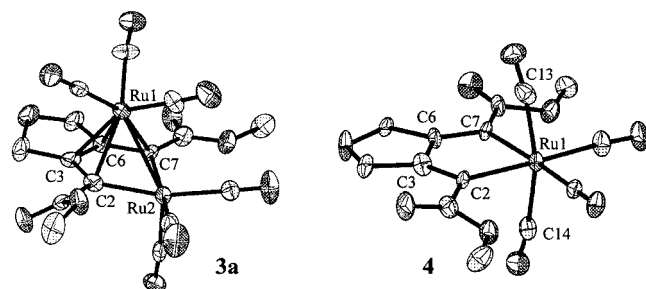
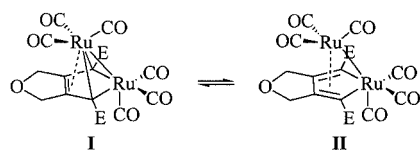


Figure 1. ORTEP diagrams of **3a** (left) and **4** (right), showing each one of two crystallographically unique molecules in the unit cell; all hydrogen atoms have been omitted for clarity

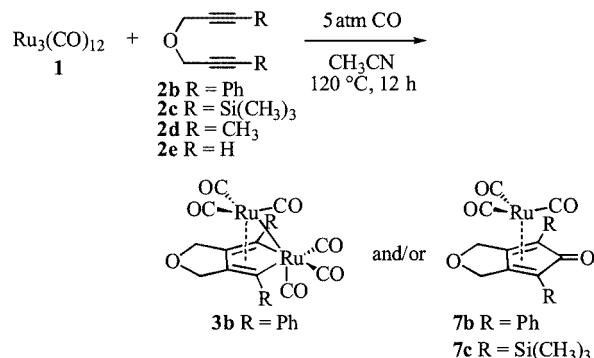


Scheme 2. Two unique structures of dinuclear ruthenabicyclic complex **3a** ($\text{E} = \text{CO}_2\text{CH}_3$)

tively). In contrast, the reaction of **3a** with 1 equiv. of **2a** under the same conditions did not produce the mononuclear complex **4**. In this case, **3a** and **2a** were recovered in 98 and 96% yields, respectively. These facts clearly show that the use of exactly 1 equiv. of **2a** per 2 Ru atoms is essential for the selective formation of the desired dinuclear complex.

Next, diynes **2b–e** bearing other substituents were treated with **1** (Scheme 3). The phenyl-substituted diyne **2b** was found to be a less-efficient substrate under the reaction conditions optimized with respect to **2a**, resulting in a low conversion of **1** (Table 1, run 8). The expected dinuclear complex **3b** was obtained in 20% yield. In addition to **3b**, a small amount of new product **7b** was also obtained. In its IR spectrum, a weak absorption is observed at 1635 cm^{-1} as well as sharp and strong absorptions corresponding to the carbonyl ligands at 2086 and 2031 cm^{-1} . The former can be assigned to a conjugated ketone carbonyl group. In accordance with this assignment, a peak of the conjugated ketone carbon atom is observed at $\delta = 173.42\text{ ppm}$ in the

^{13}C NMR spectrum. The absorption of the CO ligands also appears as a single peak at $\delta = 193.53\text{ ppm}$. On the basis of these spectroscopic data, **7b** was assigned to the cyclopentadienone complex depicted in Scheme 3.^[12] This assignment was further confirmed by X-ray crystallography (Figure 2). The use of 3 equiv. of **2b** improved the conversion of **1**, while the yields of both products were only slightly increased (run 9).



Scheme 3. Reactions of $[\text{Ru}_3(\text{CO})_{12}]$ (**1**) with diynes **2b–e**

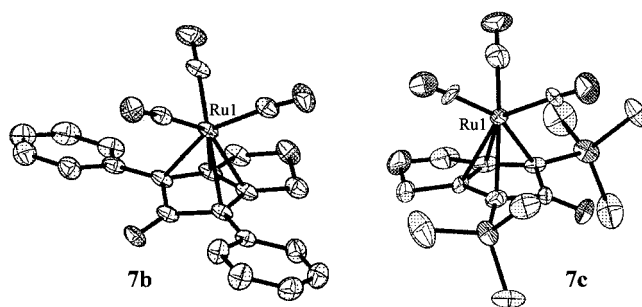


Figure 2. ORTEP diagrams of **7b** (left) and **7c** (right); all hydrogen atoms have been omitted for clarity

The reaction of the trimethylsilyl-substituted diyne **2c** with **1** gave rise to a sole product (Scheme 3). Its IR spectrum shows the presence of a conjugated carbonyl group (1623 cm^{-1}) and CO ligands (2136 – 2009 cm^{-1}), and the ^{13}C NMR spectral pattern is quite similar to that of **7b**, except for the upfield signal of the TMS-substituted sp^2 -

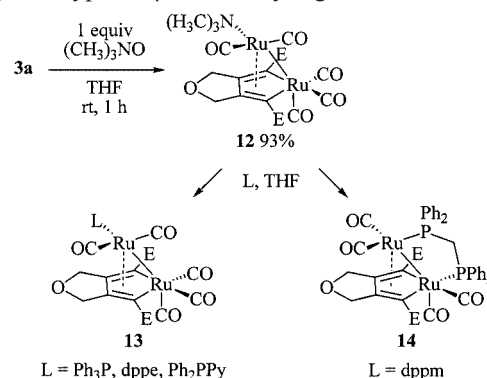
carbon atoms ($\delta = 65.78$ ppm). These spectroscopic data allowed us to assign this product as the cyclopentadienone complex **7c**. This assignment was confirmed by X-ray crystallographic analysis (Figure 2). When 1.5 equiv. of **2c** (**2c**/Ru = 1:2) was employed, **7c** was isolated in 41% yield along with 43% recovered **1** (Table 1, run 10). The increased amount of **2c** (3 equiv., **2c**/Ru atom = 1:1) raised the yield of **7c** up to 76% yield (run 11).

In contrast to the diynes **2a–c**, the diynes bearing terminal methyl substituents (**2d**) or a propargyl ether (**2e**) gave intractable product mixtures. Therefore, the electron-withdrawing methoxycarbonyl group is the optimal terminal substituent for the formation of the dinuclear ruthenacycle framework.

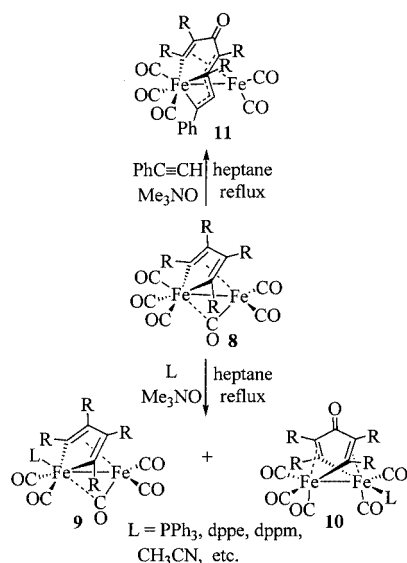
Ligand-Substitution Reactions of Dinuclear Ruthenabicyclic Complex **3a**

Having established the high-yield synthesis of the dinuclear ruthenacycle complex **3a**, we then explored its ligand-substitution reactions. Previously, Sappa, Tiripicchio, and co-workers have reported that a ferrole complex **8** reacts with various mono- and diphosphanes or nitriles in the presence of trimethylamine *N*-oxide (Me_3NO) to afford diferracycloheptadienones **10** together with simple ligand-substitution products **9** (Scheme 4).^[30] Such “flyover-bridged” complexes can be further converted into cyclopentadienone and *p*-benzoquinone derivatives. On the other hand, the reaction with phenylacetylene under the same reaction conditions resulted in the formation of a bicyclic complex **11**, probably via a “flyover” complex similar to **10**. In these cases, the ferracyclopentadiene moiety was singly cleaved at its $\text{C}_\beta\text{--C}_\beta$ bond, and subsequent CO insertion formed the “flyover-bridged” complexes. In contrast, we anticipated that such a metallacyclic ring cleavage cannot be viable for our bicyclic ruthenium complex **3a** because the ruthenacyclopentadiene moiety is stabilized by the fused

dihydrofuran ring. In fact, the treatment of **3a** with 1 equiv. of Me_3NO in THF at room temperature for 1 h afforded a trimethylamine complex **12** in 93% isolated yield (Scheme 5). Its ^1H and ^{13}C NMR spectra are very similar to those of the parent **3a** except for the additional peaks of the trimethylamine ligand. The X-ray crystallographic analysis of **12** clearly showed that the amine ligand is located on the upper ruthenium(0) center (Ru1, Figure 3). This ligand substitution regioselectivity is in contrast to that observed for the iron ferrole complex **9**, in which the newly introduced ligands are uniformly found on the metal-lacyle iron(II) center. The Ru–Ru and Ru–N bond lengths are 2.70775(19) and 2.2468(13) Å, respectively. One of the two CO ligands on the Ru1 center occupies the semi-bridge position. The $\text{C}_\alpha\text{--C}_\beta$ bonds are only slightly longer than the $\text{C}_\beta\text{--C}_\beta$ bond, indicative of the ruthenacycle moiety behaving as a typical η^4 -butadienyl ligand.



Scheme 5. Ligand-substitution reactions of dinuclear ruthenabicyclic complex **3a** ($\text{E} = \text{CO}_2\text{CH}_3$)



Scheme 4. Ligand-substitution reactions of iron ferrole complex **8** ($\text{R} = \text{C}_2\text{H}_5$)

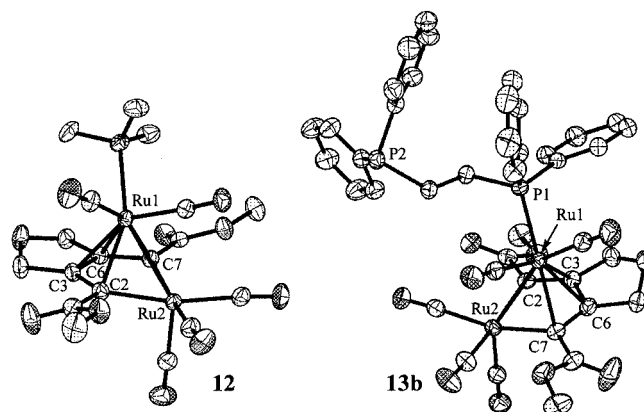


Figure 3. ORTEP diagrams of **12** (left) and **13b** (right); all hydrogen atoms have been omitted for clarity

Next, we carried out the substitutions of the amine ligand with various phosphanes, as outlined in Scheme 5 and Table 2. Upon treatment with 5 equiv. of triphenylphosphane in THF, **12** was completely consumed at room temperature after 96 h to give the expected phosphane complex **13a** ($\text{L} = \text{PPh}_3$) in 91% yield (run 1). Its ^1H NMR spectrum shows one singlet [$\delta = 3.41$ (OCH_3) ppm] and a pair of doublets [$\delta = 3.94$ and 4.65 ($-\text{CH}_2\text{OCH}_2-$) ppm] as well as the resonance of the aromatic protons ($\delta = 7.33\text{--}7.49$

ppm). The phosphorus resonance of **13a** is observed at lower field ($\delta = 41.87$ ppm) than that of free PPh_3 ($\delta = -4.94$ ppm) in the ^{31}P NMR spectrum. These facts clearly show the presence of the coordinated PPh_3 ligand in **13a**. Similarly, 1,2-bis(diphenylphosphanyl)ethane (dppe) was allowed to react with **12** at room temperature for 97 h (run 2). In the ^{31}P NMR spectrum of the obtained product both coordinated and free phosphorus peaks appear at $\delta = 40.77$ and -11.57 ppm as doublets ($J_{\text{P,P}} = 42.3$ Hz), indicative of dppe behaving as a two-electron donor ligand rather than a chelating one. This coordination mode was unambiguously confirmed by X-ray crystallography (Figure 3). The dppe ligand is located on the upper ruthenium center, and one of the remaining CO ligands occupies the semi-bridge position. The Ru1–P1 bond length is 2.3381(5) Å. At room temperature, the ligand exchange is slow and the yield of **13b** is moderate. In refluxing THF, however, the reaction is complete within 2 h, and the yield increases from 66% to 93% (run 3). Therefore, the amine complex **12** was subjected to the reaction with other phosphanes in refluxing THF.

Table 2. Reaction of trimethylamine complex **12** with phosphanes

| Run | Phosphane (equiv.) | Conditions ^[a] | Product (yield [%]) |
|-----|--|---------------------------|---------------------|
| 1 | Ph_3P (5) | room temp., 96 h | 13a (91) |
| 2 | $\text{Ph}_2\text{P}(\text{CH}_2)_2\text{PPh}_2$ (5) | room temp., 97 h | 13b (66) |
| 3 | $\text{Ph}_2\text{P}(\text{CH}_2)_2\text{PPh}_2$ (5) | reflux, 5 h | 13b (88) |
| 4 | $\text{Ph}_2\text{PCH}_2\text{PPh}_2$ (5) | reflux, 2.5 h | 14 (91) |
| 5 | Ph_2PPy (5) | reflux, 2 h | 13c (97) |

^[a] All reactions were carried out in THF under Ar.

Upon treatment with bis(diphenylphosphanyl)methane (dppm) under the same reaction conditions, **12** was consumed within 2.5 h (run 4). In contrast to the above complexes, the obtained product **14** turned out to have an unsymmetrical structure. In its ^1H NMR spectrum, the methoxy groups appear as two singlet peaks at $\delta = 3.00$ and 3.82 ppm. Similarly, the dihydrofuran ring methylene groups in an unsymmetrical environment are observed as four doublets of doublets, and the methylene protons of the dppm ligand appear as a pair of doublets of doublets [$\delta = 4.95$ ($J_{\text{H,H}} = 14$, $J_{\text{P,H}} = 22.1$ Hz) and 5.69 ($J_{\text{H,H}} = 14$, $J_{\text{P,H}} = 26.9$ Hz) ppm]. In the ^{31}P NMR spectrum, the two phosphorus atoms resonate at $\delta = 13.31$ and 15.01 ppm ($J_{\text{P,P}} = 47.9$ Hz). These data suggest that the dppm ligand forms an unsymmetrical ring. The structure of **14** was established by X-ray crystallography. As depicted in Figure 4, the dppm ligand bridges the two ruthenium centers to form a five-membered ring. The Ru2–P2 bond [2.3525(9) Å] is slightly longer than the Ru1–P1 bond [2.3276(8) Å]. The Ru–Ru bond of 2.7478(4) Å is slightly longer than those of **3a** [2.7156(7) Å] or **13b** [2.7208(2) Å].

As described above, the slight difference between dppe and dppm resulted in contrasting results. The former gave the monophosphane complex, whereas the latter directly formed the dppm-bridged complex with concomitant extrusion of 1 CO ligand. In this context, we further examined whether a similar dppe-bridged complex can be formed

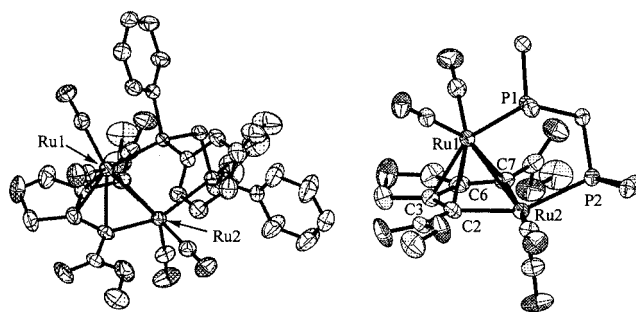
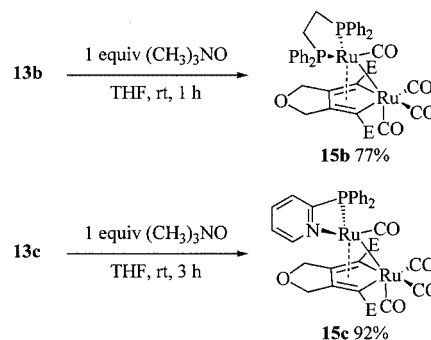


Figure 4. ORTEP diagrams of **14**; all hydrogen atoms and phenyl rings (right) have been omitted for clarity

when **13b** is treated with Me_3NO . The isolated **13b** was allowed to react with 1 equiv. of Me_3NO in THF at ambient temperature for 1 h to afford a new complex **15b** (Scheme 6). Its ^{31}P NMR spectrum, however, shows only one singlet signal at $\delta = 68.60$ ppm, indicative of the dppe ligand forming a symmetrical chelate ring. The ^1H NMR spectrum also revealed its symmetrical structure: only one methoxy signal and a pair of doublets corresponding to the methylene protons on the dihydrofuran ring are observed together with the absorptions of the benzene rings and the ethylene tether of dppe. The detailed structure of **15b** was confirmed by an X-ray crystallographic analysis (Figure 5). In contrast to **14**, both phosphorus atoms of dppe are located on the Ru1 center, and the remaining CO ligand on Ru1 occupies the semi-bridge position. The Ru–P bonds of 2.3099(16) and 2.3125(7) Å are slightly shorter than that of the parent **13b**. Consequently, the difference in the P–P distances of these two bis(phosphane) ligands alters the coordination mode from the bridge-type for dppm to the chelating one for dppe.



Scheme 6. Reactions of dinuclear ruthenabicyclic phosphane complexes **13b** and **13c** with $(\text{CH}_3)_3\text{NO}$ (E = CO_2CH_3)

In addition to the above bis(phosphanes), a P–N ligand, Ph_2PPy (Py = 2-pyridyl), was also subjected to the ligand-substitution reaction with **12** (Table 3, run 5). As a result, Ph_2PPy behaved as a monophosphane ligand to give **13c** in 97% yield. In a similar manner to **15b**, a P–N chelate complex **15c** was obtained from **13c** in 92% yield (Scheme 6). The detailed structural data for these complexes were obtained by X-ray crystallography (Figure 6). The Ru–P bond is shortened from 2.3603(9) Å for **13c** to 2.3065(15)

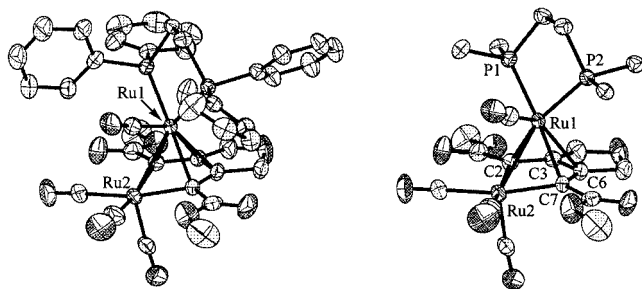


Figure 5. ORTEP diagrams of **15b**; all hydrogen atoms and phenyl rings (right) have been omitted for clarity

Å for **15c**. The Ru–Ru distance also decreases, from 2.7060(4) Å to 2.6774(6) Å, upon formation of the P–N chelate ring. The Ru1–N bond length is 2.152(5) Å.

Table 3. Comparison of average bond lengths [Å] of dinuclear ruthenacycle complexes

| | 3a(A) | 3a(B) | 12 | 13b | 13c | 14 | 15b | 15c | 16(A) | 16(B) |
|---|-------|-------|-------|-------|-------|-------|-------|-------|-------|-------|
| a | 2.716 | 2.718 | 2.708 | 2.721 | 2.706 | 2.748 | 2.704 | 2.677 | 2.729 | 2.729 |
| b | 2.088 | 2.105 | 2.105 | 2.099 | 2.103 | 2.102 | 2.086 | 2.106 | 2.171 | 2.135 |
| c | 1.473 | 1.372 | 1.424 | 1.414 | 1.418 | 1.418 | 1.427 | 1.431 | 1.380 | 1.416 |
| d | 1.351 | 1.456 | 1.402 | 1.428 | 1.451 | 1.413 | 1.400 | 1.397 | 1.473 | 1.397 |
| e | 2.246 | 2.227 | 2.209 | 2.274 | 2.249 | 2.249 | 2.230 | 2.198 | 2.198 | 2.187 |
| f | 2.239 | 2.264 | 2.304 | 2.278 | 2.291 | 2.248 | 2.311 | 2.259 | 2.298 | 2.297 |

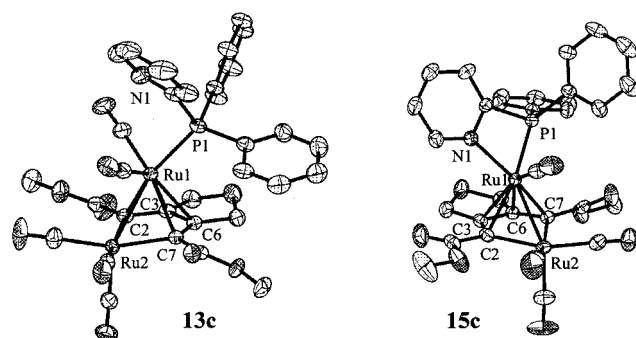
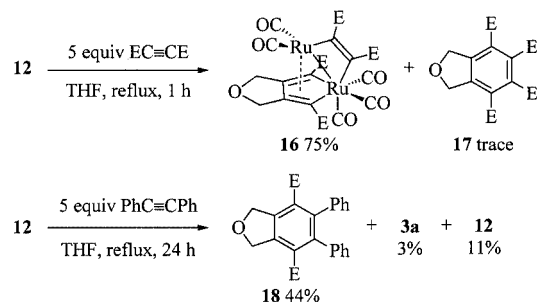


Figure 6. ORTEP diagrams of **13c** (left) and **15c** (right); all hydrogen atoms have been omitted for clarity

Reaction of Dinuclear (Amine)ruthenabicyclic Complex **12** with Alkynes

As mentioned above, metallacyclopentadiene complexes have been investigated as intermediates in alkyne cyclotrimerizations.^[1] Ferrole-type cobalt complexes have also been considered to be intermediates for [Co₂(CO)₆]-mediated alkyne cyclotrimerizations.^[5f] In this respect, dicobalt complexes bearing a “flyover” hexatrienyl ligand have been obtained from the reaction of (cobaltacyclopentadiene)cobalt complexes with alkynes.^[13] In addition, the reaction of a dinuclear cobaltacyclopentadiene complex derived from an amine-tethered diyne with phenylacetylene has

been reported to give a fused benzene in high yield.^[9a] With these facts in mind, we finally explored the reactivity of the amine complex **12** toward monoalkynes. At the outset, **12** was treated with 5 equiv. of dimethyl acetylenedicarboxylate (DMAD) in refluxing THF for 1 h (Scheme 7). As a result, a new ruthenacycle complex **16** was obtained together with trace amounts of the [2+2+2] cycloadduct **17** between the diyne **2a** and DMAD.^{[10c][10d]} The ¹H NMR analysis of **16** disclosed that the complex consists of the symmetrical ruthenacycle moiety and the unsymmetrically coordinated DMAD fragment. The methoxy and methylene protons of the ruthenacycle appear as one singlet (δ = 3.68 ppm) and two doublet peaks [δ = 4.84 and 5.06 ($J_{\text{H,H}}$ = 14.7 Hz) ppm], respectively, whereas the methoxy protons of DMAD resonate at δ = 3.84 and 3.89 ppm. Similarly, the ¹³C NMR spectrum shows 3 and 4 sp²-carbon signals for the ruthenacycle (δ = 169.81, 155.07, and 147.95 ppm) and the DMAD ligand (δ = 171.58, 165.96, 127.31, and 88.77 ppm), respectively. The structure of **16** was finally determined by X-ray crystallography (Figure 7). The unit cell contains two crystallographically unique molecules **16(A)** and **16(B)**. DMAD bridges two ruthenium centers in a “parallel” μ - η^2 fashion. The μ -alkyne bond lengths are 1.337(12) and 1.294(12) Å, and the Ru–C_{alkyne} bond lengths range from 2.028(8) to 2.224(9) Å. These bond lengths are similar to those of previously reported (μ -alkyne)diruthenium complexes.^[14] The Ru–Ru distances of 2.7289(7) Å and 2.7293(7) Å, similar to those of the above dinuclear ruthenacycle complexes [2.7039(7)–2.7478(4) Å], show the existence of a metal–metal bond. The lengths of the Ru–C_{alkyne} bonds as well as the Ru2–C2 or the Ru2–C7 bonds [2.082(8)–2.191(8) Å] are very similar to those of typical Ru–sp²-C single bonds.^[11] Thus, the formal oxidation state of the Ru1 and Ru2 centers can be regarded as +1 and +3, respectively. According to this analysis, we can conclude that the dinuclear (μ -alkyne)ruthenabicyclic complex **16** is formed by a dinuclear oxidative addition of DMAD onto the ferrole-type dinuclear framework of **12**.



Scheme 7. Reactions of dinuclear (trimethylamine)ruthenacycle complex **12** with DMAD and diphenylacetylene (E = CO₂CH₃)

The novel (μ -alkyne)ruthenacycle complex **16** seemed to be an intermediate for the formation of **17**. Indeed, upon heating **16** in refluxing THF for 24 h, compound **17** was obtained in 11% yield, although 50% of starting **16** was recovered intact. A small amount of the hexacarbonyl complex **3a** was also detected (5%). The highly electron-de-

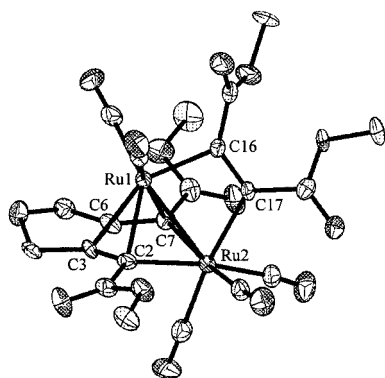


Figure 7. ORTEP diagrams of **16**, showing one of two crystallographically unique molecules in the unit cell; all hydrogen atoms have been omitted for clarity

ficient DMAD is essential for the formation of a μ -alkyne complex such as **16**. The reaction with electronically neutral diphenylacetylene afforded a coupling adduct **18** in 44% yield as well as the recovered **12** and trace amounts of **3a** (Scheme 7). Methyl propiolate never gave the corresponding complex because of its self-cyclotrimerization leading to 1,2,4- and 1,3,5-tris(methoxycarbonyl)benzenes. In contrast to our previous catalytic systems involving mononuclear ruthenacyclic intermediates,^[8] the present dinuclear complex is less effective for the [2+2+2] cycloaddition due to the stabilization of the ruthenacycle moiety by coordination to the additional ruthenium center.

Conclusion

In conclusion, the diyne diester **2a** proved to be a suitable precursor for the synthesis of the dinuclear ruthenacyclic complex **3a**. The ratio of **2a**/Ru turned out to be critical as an excess of **2a** decreased the yield of **3a** because of the concomitant formation of the mononuclear ruthenacycle complex **4**, which is the precursor of **3a**. On the other hand, the diphenyldiyne **2b** gave the cyclopentadienone complex **7b** together with the desired ruthenacycle complex **3b**, and the disilyldiyne **2c** exclusively afforded the cyclopentadienone complex **7c** in good yield.

The treatment of the ruthenacycle complex **3a** with Me_3NO gave the mono(trimethylamine) complex **12**, which was further converted into various phosphane complexes upon reaction with phosphanes in refluxing THF. Among the bidentate phosphane ligands used, only dppm afforded the bridging diphosphane complex **14** directly. In contrast, the initially formed monodentate phosphane complexes of dppe and PyPPh_2 were treated with Me_3NO to give the P-P and P-N chelate complexes **15b** and **15c**, respectively.

The reaction of **12** with DMAD gave the novel μ - η^2 -alkyne complex **16** together with the [2+2+2] cycloadduct **17**. The highly electron-deficient character of DMAD is imperative for the formation of the μ -alkyne complex; methyl propiolate and diphenylacetylene gave no corresponding μ -alkyne complexes.

Experimental Section

General Remarks: Flash chromatography was performed with a silica gel column (Merck Silica gel 60) eluting with a mixture of solvents (hexane/EtOAc). ^1H and ^{13}C NMR spectra were obtained for samples in CDCl_3 solution at 25 °C with a Varian Mercury 300 spectrometer. ^1H NMR chemical shifts are reported in δ units, in ppm relative to the singlet at $\delta = 7.26$ ppm for chloroform. ^{13}C and ^{31}P NMR spectra were fully decoupled and are reported in terms of chemical shift (δ , ppm) relative to the triplet at $\delta = 77.0$ ppm for CDCl_3 or H_4PO_4 (85% in H_2O) as external standard, respectively. Coupling constants are reported in Hz. Infrared spectra were recorded for CHCl_3 sample solutions in 0.2-mm path-length sodium chloride cavity cells with a JASCO FT/IR-230 spectrometer. Elemental analyses were performed by the Microanalytical Center of Kyoto University. Melting points were obtained in capillary tubes and are uncorrected. Toluene and acetonitrile were dried with CaH_2 and distilled. THF was dried with benzophenone ketyl, and distilled.

Typical Procedure for the Reaction of $[\text{Ru}_3(\text{CO})_{12}]$ with Diynes. Synthesis of Dinuclear Ruthenacycle Complex **3a from $[\text{Ru}_3(\text{CO})_{12}]$ and Diyne **2a**:** A glass tube (28 mm o.d.) fitted with a stirring bar was charged with $[\text{Ru}_3(\text{CO})_{12}]$ (128.0 mg, 0.20 mmol) and acetonitrile (2 mL) and saturated with CO. The tube was placed in a 100-mL stainless steel autoclave. The reactor was pressurized by CO to 5 atm. The contents were stirred at ambient temperature for 10 min, and then the pressurized CO was purged under a hood. A solution of diyne **2a** (63.4 mg, 0.30 mmol) in acetonitrile (3 mL) was added to this tube with a syringe, at ambient temperature. The reactor was pressurized again with CO to 5 atm. The contents were stirred at 120 °C for 12 h, and cooled to ambient temperature. After purging the excess CO under a fume hood, the reaction mixture was concentrated in vacuo. The residue was chromatographed on silica gel using hexane/EtOAc (10:1) as an eluent to give **3a** (151.1 mg, 87%) as a yellow solid: M.p. 110.0–111.0 °C. IR (CHCl_3 , 25 °C): $\tilde{\nu} = 2096, 2068, 2062, 2029, 2011, 1689 \text{ cm}^{-1}$. ^1H NMR (300 MHz, CDCl_3 , 25 °C): $\delta = 3.68$ (s, 6 H), 4.80 (dd, $J_{\text{H,H}} = 15.3, 2.4 \text{ Hz}$, 2 H), 5.08 (dd, $J_{\text{H,H}} = 15.3, 2.4 \text{ Hz}$, 2 H) ppm. ^{13}C NMR (75 MHz, CDCl_3 , 25 °C): $\delta = 52.28, 70.31, 127.62, 137.23, 172.38, 192.21, 193.60, 194.37 \text{ ppm}$. $\text{C}_{16}\text{H}_{10}\text{O}_1\text{Ru}_2$ (580.38): calcd. C 33.11, H 1.74; found C 33.11, H 1.91. Other reactions of $\text{Ru}_3(\text{CO})_{12}$ with diynes **2a–c** were carried out in a similar way under the conditions summarized in Tables 1 and 2.

Mononuclear Ruthenacycle Complex **4:** M.p. 128.5–130.0 °C. IR (CHCl_3 , 25 °C): $\tilde{\nu} = 2145, 2073, 1676 \text{ cm}^{-1}$. ^1H NMR (300 MHz, CDCl_3 , 25 °C): $\delta = 3.75$ (s, 6 H), 4.65 (s, 4 H) ppm. ^{13}C NMR (75 MHz, CDCl_3 , 25 °C): $\delta = 51.98, 70.62, 133.66, 171.08, 177.11, 186.32, 189.82 \text{ ppm}$. $\text{C}_{14}\text{H}_{10}\text{O}_9\text{Ru}$ (423.29): calcd. C 39.72, H 2.38; found C 39.69, H 2.48.

Dinuclear Ruthenacycle Complex **3b:** M.p. 158.0–158.5 °C. IR (CHCl_3 , 25 °C): $\tilde{\nu} = 2081, 2052, 2010 \text{ cm}^{-1}$. ^1H NMR (300 MHz, CDCl_3 , 25 °C): $\delta = 4.43$ (dd, $J_{\text{H,H}} = 13.8, 1.8 \text{ Hz}$, 2 H), 5.15 (dd, $J_{\text{H,H}} = 13.8, 1.8 \text{ Hz}$, 2 H), 7.00–7.04 (m, 4 H), 7.11–7.17 (m, 2 H), 7.21–7.27 (m, 4 H) ppm. ^{13}C NMR (75 MHz, CDCl_3 , 25 °C): $\delta = 69.50, 126.57, 127.03, 128.13, 135.91, 147.15, 154.41, 193.49, 195.99, 198.52 \text{ ppm}$. $\text{C}_{24}\text{H}_{14}\text{O}_7\text{Ru}_2$ (616.50): calcd. C 46.76, H 2.29; found C 46.80, H 2.48.

Cyclopentadienone Complex **7b:** M.p. 200 °C (decomp). IR (CHCl_3 , 25 °C): $\tilde{\nu} = 2086, 2031, 1635 \text{ cm}^{-1}$. ^1H NMR (300 MHz, CDCl_3 , 25 °C): $\delta = 5.11$ (dd, $J_{\text{H,H}} = 13.5, 2.4 \text{ Hz}$, 2 H), 5.27 (dd, $J_{\text{H,H}} = 13.5, 2.4 \text{ Hz}$, 2 H), 7.26–7.32 (m, 2 H), 7.35–7.41 (m, 4 H),

7.80–7.85 (m, 4 H) ppm. ^{13}C NMR (75 MHz, CDCl_3 , 25 °C): δ = 68.77, 75.26, 103.37, 126.96, 127.63, 128.76, 132.17, 173.42, 193.53 ppm. $\text{C}_{22}\text{H}_{14}\text{O}_3\text{Ru}$ (459.41): calcd. C 57.52, H 3.07; found C 57.37, H 3.35.

Cyclopentadienone Complex 7c: M.p. 143.5–144.5 °C. IR (CHCl_3 , 25 °C): $\tilde{\nu}$ = 2136, 2084, 2064, 2028, 2009, 1623 cm^{-1} . ^1H NMR (300 MHz, CDCl_3 , 25 °C): δ = 0.25 (s, 18 H), 4.77 (s, 4 H) ppm. ^{13}C NMR (75 MHz, CDCl_3 , 25 °C): δ = –0.29, 65.78, 68.14, 114.07, 185.48, 193.67 ppm. $\text{C}_{16}\text{H}_{22}\text{O}_5\text{RuSi}_2$ (451.58): calcd. C 42.55, H 4.91; found C 42.39, H 4.83.

Synthesis of Trimethylamine Complex 12: $\text{Me}_3\text{NO}/2\text{H}_2\text{O}$ (24.6 mg, 0.22 mmol) was added to a degassed solution of **3a** (120.6 mg, 0.21 mmol) in THF (10 mL), and the reaction mixture was stirred for 1 h at ambient temperature under Ar. The solvent was removed in vacuo, and the residue was chromatographed on silica gel using hexane/EtOAc (2:1) as eluent to give **12** (117.8 mg, 93%) as a dark-red solid. M.p. 120 °C (decomp). IR (CHCl_3 , 25 °C): $\tilde{\nu}$ = 2077, 2006, 1952, 1682 cm^{-1} . ^1H NMR (300 MHz, CDCl_3 , 25 °C): δ = 2.69 (s, 9 H), 3.60 (s, 6 H), 4.76 (dd, $J_{\text{H,H}}$ = 15.9, 2.7 Hz, 2 H), 5.09 (dd, $J_{\text{H,H}}$ = 15.9, 2.7 Hz, 2 H) ppm. ^{13}C NMR (75 MHz, CDCl_3 , 25 °C): δ = 51.62, 59.78, 70.43, 120.84, 137.03, 174.69, 194.33, 195.62, 201.48 ppm. $\text{C}_{18}\text{H}_{19}\text{NO}_{10}\text{Ru}_2$ (611.48): calcd. C 35.36, H 3.13, N 2.29; found C 35.28, H 3.10, N 2.24.

Typical Procedure for the Reaction of 12 with Phosphanes: Synthesis of dppe Complex 13b from 12: A degassed solution of **12** (122.4 mg, 0.20 mmol) and dppe (398.6 mg, 1.0 mmol) in THF (10 mL) was refluxed under N_2 for 5 h. The reaction mixture was concentrated in vacuo, and the residue was chromatographed on silica gel using hexane/EtOAc (8:1–4:1) as eluent to give **13b** (166.9 mg, 93%) as a yellow solid. M.p. 143.5–144.0 °C. IR (CHCl_3 , 25 °C): $\tilde{\nu}$ = 2077, 2008, 1683 cm^{-1} . ^1H NMR (300 MHz, CDCl_3 , 25 °C): δ = 1.92–2.04 (br. m, 2 H), 2.32–2.46 (br. m, 2 H), 3.47 (s, 6 H), 3.98 (d, $J_{\text{H,H}}$ = 13.2 Hz, 2 H), 4.67 (d, $J_{\text{H,H}}$ = 13.2 Hz, 2 H), 7.18–7.48 (m, 20 H) ppm. ^{13}C NMR (75 MHz, CDCl_3 , 25 °C): δ = 22.13 (d, $J_{\text{P,C}}$ = 15.9 Hz), 28.03 (d, $J_{\text{P,C}}$ = 19.4 Hz), 51.73, 69.19, 128.39–128.74 (m), 130.68 (d, $J_{\text{P,C}}$ = 2.3 Hz), 131.54, 132.10 (d, $J_{\text{P,C}}$ = 10.2 Hz), 132.35 (d, $J_{\text{P,C}}$ = 18.2 Hz), 134.71, 136.99 (d, $J_{\text{P,C}}$ = 12 Hz), 173.14, 194.67, 195.36, 201.40 (d, $J_{\text{P,C}}$ = 13.1 Hz) ppm. ^{31}P NMR (121.5 MHz, CDCl_3 , 25 °C): δ = –11.57 (d, $J_{\text{P,P}}$ = 42.3 Hz), 40.77 (d, $J_{\text{P,P}}$ = 42.3 Hz) ppm. $\text{C}_{41}\text{H}_{34}\text{O}_{10}\text{P}_2\text{Ru}_2$ (950.79): calcd. C 51.79, H 3.60; found C 51.91, H 3.50. The reactions of **12** with other phosphanes were carried out in a similar way under the conditions summarized in Table 3.

Complex 13a: M.p. 171.0–172.0 °C. IR (CHCl_3 , 25 °C): $\tilde{\nu}$ = 2077, 2013, 1989, 1961, 1683 cm^{-1} . ^1H NMR (300 MHz, CDCl_3 , 25 °C): δ = 3.41 (s, 6 H), 3.94 (d, $J_{\text{H,H}}$ = 13.4 Hz, 2 H), 4.65 (d, $J_{\text{H,H}}$ = 13.4 Hz, 2 H), 7.33–7.49 (m, 15 H) ppm. ^{13}C NMR (75 MHz, CDCl_3 , 25 °C): δ = 51.62, 69.18, 127.85 (d, $J_{\text{P,C}}$ = 6.8 Hz), 128.39 (d, $J_{\text{P,C}}$ = 10.3 Hz), 130.64 (d, $J_{\text{P,C}}$ = 2.3 Hz), 132.26, 132.91, 133.07 (d, $J_{\text{P,C}}$ = 11.4 Hz), 135.56, 173.21, 194.70, 195.45, 200.95 (d, $J_{\text{P,C}}$ = 13.7 Hz) ppm. ^{31}P NMR (121.5 MHz, CDCl_3 , 25 °C): δ = 41.87 ppm. $\text{C}_{33}\text{H}_{25}\text{O}_{10}\text{PRu}_2$ (814.66): calcd. C 48.65, H 3.09; found C 48.61, H 3.16.

Complex 13c: M.p. 153.5–154.0 °C. IR (CHCl_3 , 25 °C): $\tilde{\nu}$ = 2075, 2014, 1987, 1682 cm^{-1} . ^1H NMR (300 MHz, CDCl_3 , 25 °C): δ = 3.41 (s, 6 H), 4.06 (d, $J_{\text{H,H}}$ = 12.9 Hz, 2 H), 4.71 (dd, $J_{\text{H,H}}$ = 12.9, 1.5 Hz, 2 H), 7.20–7.30 (m, 2 H), 7.40–7.52 (m, 10 H), 7.63 (ddt, $J_{\text{H,H}}$ = 7.8, 3.6, 2.1 Hz, 1 H), 8.77–8.81 (m, 1 H) ppm. ^{13}C NMR (75 MHz, CDCl_3 , 25 °C): δ = 51.55, 69.34, 123.91 (d, $J_{\text{P,C}}$ = 2.3 Hz), 126.85 (d, $J_{\text{P,C}}$ = 18.8 Hz), 128.38 (d, $J_{\text{P,C}}$ = 10.3 Hz), 130.71, 130.81 (d, $J_{\text{P,C}}$ = 2.9 Hz), 131.32, 133.62 (d, $J_{\text{P,C}}$ =

11.4 Hz), 134.57, 135.56 (d, $J_{\text{P,C}}$ = 6.8 Hz), 150.24 (d, $J_{\text{P,C}}$ = 18.2 Hz), 158.41, 159.42, 173.36, 195.07, 195.80, 200.18 (d, $J_{\text{P,C}}$ = 13.7 Hz) ppm. ^{31}P NMR (121.5 MHz, CDCl_3 , 25 °C): δ = 46.12 ppm. $\text{C}_{32}\text{H}_{24}\text{NO}_{10}\text{PRu}_2$ (815.65): calcd. C 47.12, H 2.97, N 1.72; found C 46.99, H 3.13, N 1.69.

Complex 14: M.p. 235 °C (decomp). IR (CHCl_3 , 25 °C): $\tilde{\nu}$ = 2032, 2010, 1977, 1941, 1682 cm^{-1} . ^1H NMR (300 MHz, CDCl_3 , 25 °C): δ = 3.00 (s, 3 H), 3.82 (s, 3 H), 4.39 (d, $J_{\text{H,H}}$ = 13.2 Hz, 1 H), 4.69 (d, $J_{\text{H,H}}$ = 12.6 Hz, 1 H), 4.95 (dd, $J_{\text{P,H}}$ = 22.1, $J_{\text{H,H}}$ = 14 Hz, 1 H), 4.95 (d, $J_{\text{H,H}}$ = 13.2 Hz, 1 H), 5.18 (dd, $J_{\text{H,H}}$ = 12.6, 3.9 Hz, 1 H), 5.69 (dd, $J_{\text{P,H}}$ = 26.9, $J_{\text{H,H}}$ = 14 Hz, 1 H), 6.72–6.78 (m, 2 H), 6.95–7.11 (m, 3 H), 7.32–7.67 (m, 13 H), 7.94–8.02 (m, 2 H) ppm. ^{13}C NMR (75 MHz, CDCl_3 , 25 °C): δ = 48.41 (dd, $J_{\text{P,C}}$ = 29, 18.2 Hz), 51.18, 51.66, 69.11, 71.07, 114.52 (dd, $J_{\text{P,C}}$ = 14.3, 5.2 Hz), 119.73 (d, $J_{\text{P,C}}$ = 5.7 Hz), 127.70–129.83 (m), 131.47 (d, $J_{\text{P,C}}$ = 2.3 Hz), 132.06 (d, $J_{\text{P,C}}$ = 13.1 Hz), 135.47–136.16 (m), 136.88, 137.22–137.45 (m), 140.89, 141.63, 143.39 (d, $J_{\text{P,C}}$ = 14.8 Hz), 143.99 (d, $J_{\text{P,C}}$ = 14.8 Hz), 174.80, 176.47, 176.52, 195.77 (d, $J_{\text{P,C}}$ = 9.7 Hz), 199.10 (d, $J_{\text{P,C}}$ = 12.5 Hz), 200.32 (d, $J_{\text{P,C}}$ = 9.1 Hz), 201.75 (dd, $J_{\text{P,C}}$ = 10.8, 9.1 Hz) ppm. ^{31}P NMR (121.5 MHz, CDCl_3 , 25 °C): δ = 13.31 (d, $J_{\text{P,P}}$ = 47.9 Hz), 15.01 (d, $J_{\text{P,P}}$ = 47.9 Hz) ppm. $\text{C}_{39}\text{H}_{32}\text{O}_9\text{P}_2\text{Ru}_2$ (908.75): calcd. C 51.55, H 3.55; found C 51.27, H 3.62.

Typical Procedure for Reaction of Phosphane Complexes 13b,c with Me_3NO . Synthesis of dppe Chelate Complex 15b: $\text{Me}_3\text{NO}/2\text{H}_2\text{O}$ (12.4 mg, 0.11 mmol) was added to a degassed solution of **13b** (95.0 mg, 0.10 mmol) in THF (25 mL) and the reaction mixture was stirred at ambient temperature under Ar for 1 h. The solvent was removed in vacuo, and the residue was chromatographed on silica gel using hexane/EtOAc (2.5:1–1:1) as eluent to give **15b** (71.0 mg, 77%) as a yellow solid. M.p. 190 °C (decomp). IR (CHCl_3 , 25 °C): $\tilde{\nu}$ = 2063, 1996, 1975, 1929, 1673 cm^{-1} . ^1H NMR (300 MHz, CDCl_3 , 25 °C): δ = 2.40–2.65 (m, 4 H), 3.18 (s, 6 H), 3.47 (d, $J_{\text{H,H}}$ = 12.6 Hz, 2 H), 4.43 (dd, $J_{\text{H,H}}$ = 12.6, 2.4 Hz, 2 H), 7.19–7.26 (m, 4 H), 7.38–7.48 (m, 12 H), 7.64–7.72 (m, 4 H) ppm. ^{13}C NMR (75 MHz, CDCl_3 , 25 °C): δ = 30.68 (dd, $J_{\text{P,C}}$ = 23.3, 22.2 Hz), 50.83, 68.75, 124.38 (t, $J_{\text{P,C}}$ = 8.5 Hz), 128.15 (t, $J_{\text{P,C}}$ = 6.8 Hz), 128.21 (t, $J_{\text{P,C}}$ = 6.8 Hz), 130.20, 130.52, 131.81 (t, $J_{\text{P,C}}$ = 5.7 Hz), 132.77 (d, $J_{\text{P,C}}$ = 3.5 Hz), 133.40 (t, $J_{\text{P,C}}$ = 5.1 Hz), 133.65, 133.95, 174.70, 196.34, 197.30, 203.98 (t, $J_{\text{P,C}}$ = 13.7 Hz) ppm. ^{31}P NMR (121.5 MHz, CDCl_3 , 25 °C): δ = 68.60 ppm. $\text{C}_{40}\text{H}_{34}\text{O}_9\text{P}_2\text{Ru}_2$ (922.78): calcd. C 52.06, H 3.71; found C 51.96, H 3.71.

Complex 15c: M.p. 175.0–176.0 °C. IR (CHCl_3 , 25 °C): $\tilde{\nu}$ = 2063, 1994, 1971, 1923, 1670 cm^{-1} . ^1H NMR (300 MHz, CDCl_3 , 25 °C): δ = 3.21 (dt, $J_{\text{H,H}}$ = 12.5, 1.8 Hz, 1 H), 3.32 (s, 3 H), 3.69 (s, 3 H), 4.33 (dd, $J_{\text{H,H}}$ = 13.5, 2.1 Hz, 1 H), 4.51 (ddt, $J_{\text{H,H}}$ = 12.5, 3.6, 1.8 Hz, 1 H), 4.84 (dt, $J_{\text{H,H}}$ = 13.5, 1.8 Hz, 1 H), 6.94–7.02 (m, 2 H), 7.32–7.47 (m, 5 H), 7.55–7.61 (m, 3 H), 7.82–7.93 (m, 3 H), 8.04 (dd, $J_{\text{H,H}}$ = 5.4, 0.8 Hz, 1 H) ppm. ^{13}C NMR (75 MHz, CDCl_3 , 25 °C): δ = 50.72, 51.56, 68.18, 70.13, 113.83 (d, $J_{\text{P,C}}$ = 19.9 Hz), 118.81 (d, $J_{\text{P,C}}$ = 3.4 Hz), 126.51 (d, $J_{\text{P,C}}$ = 2.3 Hz), 127.14, 127.99 (d, $J_{\text{P,C}}$ = 2.9 Hz), 128.34, 128.75 (d, $J_{\text{P,C}}$ = 10.8 Hz), 128.91, 129.07 (d, $J_{\text{P,C}}$ = 10.8 Hz), 129.21, 130.71 (d, $J_{\text{P,C}}$ = 2.3 Hz), 131.21 (d, $J_{\text{P,C}}$ = 11.3 Hz), 132.03 (d, $J_{\text{P,C}}$ = 2.3 Hz), 134.40 (d, $J_{\text{P,C}}$ = 13.1 Hz), 134.66, 137.26 (d, $J_{\text{P,C}}$ = 3.5 Hz), 152.19 (d, $J_{\text{P,C}}$ = 15.4 Hz), 172.40, 173.10, 177.13 (d, $J_{\text{P,C}}$ = 2.3 Hz), 177.39, 195.91, 197.08, 197.52, 205.02 (d, $J_{\text{P,C}}$ = 12.5 Hz) ppm. ^{31}P NMR (121.5 MHz, CDCl_3 , 25 °C): δ = –2.60 ppm. $\text{C}_{31}\text{H}_{24}\text{NO}_9\text{PRu}_2$ (787.64): calcd. C 47.27, H 3.07, N 1.78; found C 47.19, H 3.23, N 1.70.

Typical Procedure for the Reaction of 12 with Alkynes. Synthesis of DMAD Complex 16: A degassed solution of **12** (122.8 mg, 0.20 mmol) and DMAD (145.1 mg, 1.0 mmol) in THF (10 mL) was refluxed under N₂ for 1 h. The reaction mixture was concentrated in vacuo, and the residue was chromatographed on silica gel using hexane/EtOAc (8:1) as eluent to give **16** (104.7 mg, 75%) as a yellow solid. M.p. 119.0–120.0 °C. IR (CHCl₃, 25 °C): $\tilde{\nu}$ = 2113, 2056, 2009, 1704 cm⁻¹. ¹H NMR (300 MHz, CDCl₃, 25 °C): δ = 3.68 (s, 6 H), 3.84 (s, 3 H), 3.89 (s, 3 H), 4.84 (d, $J_{\text{H,H}}$ = 14.7 Hz, 2 H), 5.06 (d, $J_{\text{H,H}}$ = 14.7 Hz, 2 H) ppm. ¹³C NMR (75 MHz, CDCl₃,

25 °C): δ = 52.73, 53.19, 71.64, 88.77, 127.31, 147.95, 155.07, 165.96, 169.81, 171.58, 187.87, 188.83, 194.10 ppm. C₂₁H₁₆O₁₄Ru₂ (694.48): calcd. C 36.32, H 2.32; found C 36.17, H 2.32. The reactions of **12** with other alkynes were carried out in a similar way.

Cycloadduct 18: M.p. 150.0–151.0 °C. IR (CHCl₃, 25 °C): $\tilde{\nu}$ = 1723 cm⁻¹. ¹H NMR (300 MHz, CDCl₃, 25 °C): δ = 3.49 (s, 6 H), 5.31 (s, 4 H), 6.90–6.96 (m, 4 H), 7.09–7.13 (m, 6 H). ¹³C NMR (75 MHz, CDCl₃, 25 °C): δ = 52.01, 73.80, 126.65, 127.16, 128.28, 129.61, 138.39, 139.29, 141.07, 167.33 ppm. MS (EI): m/z (%) =

Table 4. Selected crystallographic data and collection parameters for **3a**, **4**, **7b**, **7c**, and **12**

| | 3a | 4 | 7b | 7c | 12 |
|---|---|---|---|--|--|
| Empirical formula | C ₃₂ H ₂₀ O ₂₂ Ru ₄ | C ₂₈ H ₁₀ O ₁₈ Ru ₂ | C ₂₂ H ₁₄ O ₅ Ru | C ₁₆ H ₂₂ O ₅ RuSi ₂ | C ₁₈ H ₁₉ NO ₁₀ Ru ₂ |
| Formula mass | 1160.76 | 836.50 | 459.40 | 451.59 | 611.48 |
| Crystal system | triclinic | triclinic | monoclinic | orthorhombic | orthorhombic |
| Space group | <i>P</i> 1 | <i>P</i> 1 | <i>P</i> 2 ₁ / <i>n</i> | <i>P</i> na2 ₁ | <i>P</i> bca |
| <i>a</i> [Å] | 7.2890(4) | 7.4477(4) | 12.5010(17) | 13.5068(11) | 14.5489(7) |
| <i>b</i> [Å] | 8.4070(4) | 7.6427(4) | 11.1785(15) | 7.7041(6) | 16.5372(8) |
| <i>c</i> [Å] | 15.6155(8) | 13.9935(7) | 13.5392(18) | 19.7067(17) | 18.0212(9) |
| α [°] | 85.4440(10) | 84.6270(10) | 90 | 90 | 90 |
| β [°] | 79.6470(10) | 78.4880(10) | 96.956(3) | 90 | 90 |
| γ [°] | 86.9670(10) | 77.9490(10) | 90 | 90 | 90 |
| <i>V</i> [Å ³] | 937.61(8) | 762.17(7) | 1878.1(4) | 2050.6(3) | 4335.9(4) |
| <i>Z</i> | 1 | 1 | 4 | 4 | 8 |
| <i>D</i> _{calcd.} [Mg cm ⁻³] | 4.111 | 3.645 | 1.625 | 1.463 | 1.873 |
| μ [mm ⁻¹] | 3.339 | 2.150 | 0.866 | 0.901 | 1.447 |
| <i>F</i> (000) | 1128 | 820 | 920 | 920 | 2416 |
| Crystal size [mm] | 0.2 × 0.4 × 0.8 | 0.01 × 0.4 × 0.7 | 0.2 × 0.3 × 0.8 | 0.05 × 0.1 × 0.7 | 0.3 × 0.6 × 0.6 |
| Reflections collected | 7287 | 5879 | 14090 | 14810 | 32235 |
| Independent reflections | 5892 | 4759 | 4979 | 5170 | 5832 |
| GOF on <i>F</i> ² | 1.067 | 0.835 | 0.839 | 0.984 | 1.094 |
| <i>R</i> ^[a] | 0.0267, | 0.0258, | 0.0297, | 0.0267, | 0.0206, |
| <i>wR</i> ^[b] | 0.0714 | 0.0686 | 0.0808 | 0.0678 | 0.0557 |
| Largest diff. peak/hole [e ⁻ Å ⁻³] | 0.448/−1.362 | 0.661/−1.076 | 0.710/−1.379 | 0.761/−0.335 | 0.693/−0.499 |

[a] $R_1 = \Sigma(|F_o - F_c|)/\Sigma(F_o)$. [b] $wR = \Sigma\{[w(F_o - F_c)^2]\}/\Sigma(wF_o^2)^{1/2}$.

Table 5. Selected crystallographic data and collection parameters for **13b**, **13c**, **14**, **15b**, **15c**, and **16**

| | 13b | 13c | 14 | 15b | 15c | 16 |
|---|--|---|---|---|--|--|
| Empirical formula | C ₄₁ H ₃₄ O ₁₀ P ₂ Ru ₂ | C ₃₂ H ₂₄ NO ₁₀ PRu ₂ | C ₃₉ H ₃₂ O ₉ P ₂ Ru ₂ | C ₄₀ H ₃₄ O ₉ P ₂ Ru ₂ | C ₃₁ H ₂₄ NO ₉ PRu ₂ | C ₄₂ H ₃₂ O ₂₈ P ₂ Ru ₄ |
| Formula mass | 950.76 | 815.63 | 908.73 | 922.75 | 787.62 | 1388.96 |
| Crystal system | triclinic | triclinic | monoclinic | triclinic | monoclinic | triclinic |
| Space group | <i>P</i> 1̄ | <i>P</i> 1̄ | <i>P</i> 2 ₁ / <i>c</i> | <i>P</i> 1̄ | <i>P</i> 2 ₁ / <i>c</i> | <i>P</i> 1 |
| <i>a</i> [Å] | 11.4786(57) | 11.2420(6) | 16.9441(11) | 10.5914(10) | 14.3052(10) | 8.1357(5) |
| <i>b</i> [Å] | 11.9273(5) | 11.9006(6) | 12.7293(9) | 10.7131(10) | 20.8765(14) | 9.2184(6) |
| <i>c</i> [Å] | 15.0854(7) | 13.4346(7) | 20.2441(13) | 17.0451(17) | 11.4404(8) | 17.9529(11) |
| α [°] | 93.8670(10) | 84.7860(10) | 90 | 94.634(2) | 90 | 95.7720(10) |
| β [°] | 92.2860(10) | 72.6960(10) | 111.8660(10) | 103.678(2) | 96.981(2) | 102.8400(10) |
| γ [°] | 110.5380(10) | 85.6630(10) | 90 | 91.953(2) | 90 | 109.9680(10) |
| <i>V</i> [Å ³] | 1925.18(15) | 1706.69(15) | 4052.3(5) | 1870.2(3) | 3391.3(4) | 1210.75(13) |
| <i>Z</i> | 2 | 2 | 4 | 2 | 4 | 1 |
| <i>D</i> _{calcd.} [Mg cm ⁻³] | 1.640 | 1.587 | 1.490 | 1.639 | 1.543 | 3.810 |
| μ [mm ⁻¹] | 0.926 | 0.986 | 0.875 | 0.949 | 0.988 | 2.639 |
| <i>F</i> (000) | 956 | 812 | 1824 | 928 | 1568 | 1368 |
| Crystal size [mm] | 0.01 × 0.4 × 0.7 | 0.1 × 0.5 × 0.6 | 0.1 × 0.5 × 0.8 | 0.01 × 0.2 × 0.4 | 0.01 × 0.5 × 0.6 | 0.1 × 0.4 × 0.8 |
| Reflections collected | 15104 | 13218 | 30637 | 12716 | 25394 | 9402 |
| Independent reflections | 10090 | 8874 | 10862 | 9575 | 9036 | 7593 |
| GOF on <i>F</i> ² | 0.750 | 0.993 | 0.991 | 1.042 | 1.013 | 1.078 |
| <i>R</i> ^[a] | 0.0269, | 0.0432, | 0.0419, | 0.0687, | 0.0626, | 0.0273, |
| <i>wR</i> ^[b] | 0.0739 | 0.1572 | 0.1320 | 0.1641 | 0.2060 | 0.0735 |
| Largest diff. peak/hole [e ⁻ Å ⁻³] | 0.841/−0.443 | 4.212/−0.466 | 2.770/−0.699 | 3.386/−2.059 | 5.934/−0.584 | 0.570/−1.315 |

[a] $R_1 = \Sigma(|F_o - F_c|)/\Sigma(F_o)$. [b] $wR = \Sigma\{[w(F_o - F_c)^2]\}/\Sigma(wF_o^2)^{1/2}$.

388 (100) [M⁺], 373 (28) [M⁺ – CH₃], 356 (82) [M⁺ – HOCH₃]. C₂₄H₂₀O₅ (388.41): calcd. C 74.21, H 5.19; found C 73.97, H 5.43.

X-ray Crystallographic Determination: Single crystals suitable for X-ray analysis were obtained by recrystallization from hexane at –15 °C (**3a**), CH₂Cl₂/hexane at room temp. (**4**), EtOAc/hexane at room temp. (**7b**), EtOAc/hexane at –15 °C (**7c**), CH₂Cl₂/diethyl ether at –15 °C (**12**), diethyl ether/hexane at room temp. (**13b**), diethyl ether/hexane at room temp. (**13c**), CHCl₃/hexane at room temp. (**14**), CH₂Cl₂/hexane at room temp. (**15b**), CH₂Cl₂/diethyl ether at room temp. (**15c**), or CH₂Cl₂/hexane at 0 °C (**16**). Each crystal was mounted on a quartz fiber, and diffraction data were collected in θ ranges specified in Tables 4 and 5 at 173 K with a Bruker SMART APEX CCD diffractometer with graphite-monochromated Mo- K_{α} radiation ($\lambda = 0.71073$ Å). An absorption correction was applied using SADABS. The structure was solved by direct methods and refined by full-matrix least squares on F^2 with SHELXTL.^[15] All non-hydrogen atoms were refined with anisotropic displacement parameters. All hydrogen atoms were placed in calculated positions. Final refinement details are compiled in Tables 4 and 5. CCDC-227166 (**3a**), -227167 (**4**), -227168 (**7b**), -227169 (**7c**), -227170 (**12**), -227171 (**13b**), -227172 (**13c**), -227173 (**14**), -227174 (**15b**), -227175 (**15c**), and -227176 (**16**) contain the supplementary crystallographic data for this paper. These data can be obtained free of charge at www.ccdc.cam.ac.uk/conts/retrieving.html [or from the Cambridge Crystallographic Data Centre, 12 Union Road, Cambridge CB2 1EZ, UK; Fax: + 44-1223-336033; E-mail: deposit@ccdc.cam.ac.uk].

Acknowledgments

We gratefully acknowledge financial support (14750677) from the Ministry of Education, Culture, Sports, Science and Technology, Japan.

- [1] [1a] S. Otsuka, A. Nakamura, *Adv. Organomet. Chem.* **1976**, *14*, 245–283. [1b] N. E. Schore, *Chem. Rev.* **1988**, *88*, 1081–1119. [1c] N. E. Shore, in *Comprehensive Organic Synthesis*, vol. 5 (Eds.: B. M. Trost, I. Fleming, L. A. Paquette), Pergamon, Oxford, **1991**, p. 1129–1162. [1d] D. B. Grotjahn, in *Comprehensive Organometallic Chemistry II*, vol. 12 (Eds.: E. W. Abel, F. G. A. Stone, G. Wilkinson, L. S. Hegehus), Pergamon, Oxford, **1995**, p. 741–770. [1e] H. Bönemann, W. Brijoux, in *Transition Metals for Organic Synthesis* (Eds.: M. Beller, C. Bolm), Wiley-VCH, Weinheim, **1998**, vol. 1, p. 114–135.
- [2] [2a] L. R. Bateman, P. M. Maitlis, L. F. Dahl, *J. Am. Chem. Soc.* **1969**, *91*, 7292–7300. [2b] J. Levisalles, F. Rose-Munch, H. Rudler, *J. Chem. Soc., Chem. Commun.* **1981**, 1057–1059. [2c] H. Yamazaki, K. Yasufuku, Y. Wakatsuki, *Organometallics* **1983**, *2*, 726–732, and references cited therein. [2d] H. Yamazaki, Y. Wakatsuki, *J. Organomet. Chem.* **1984**, *272*, 251–263. [2e] S. B. Colbran, B. H. Robinson, J. Simpson, *Organometallics* **1985**, *4*, 1594–1601. [2f] K. Sünkel, *J. Organomet. Chem.* **1990**, *391*, 247–257. [2g] R. D. Adams, I. Arafat, G. Chen, J.-C. Lii, J.-G. Wang, *Organometallics* **1990**, *9*, 2350–2357. [2h] J. Müller, T. Akhnoukh, J. Pickardt, M. Siewing, B. Westphal, *J. Organomet. Chem.* **1993**, *459*, 325–333. [2i] F.-E. Hong, I.-R. Lue, S.-C. Lo, C.-C. Lin, *J. Organomet. Chem.* **1995**, *495*, 97–101. [2j] H. Matsuzaka, K. Ichikawa, T. Ishioka, H. Sato, T. Okubo, T. Ishii, M. Yamashita, M. Kondo, S. Kitagawa, *J. Organomet. Chem.* **2000**, *596*, 121–129.
- [3] [3a] W. Hübel, E. H. Braye, *J. Inorg. Nucl. Chem.* **1959**, *10*, 250–268. [3b] E. Weiss, W. Hübel, R. Merényi, *Chem. Ber.* **1962**, *95*, 1155–1169. [3c] W. Hübel, R. Merényi, *Chem. Ber.* **1963**, *96*, 930–943. [3d] R. B. King, I. Haiduc, C. W. Eavenson, *J. Am. Chem. Soc.* **1973**, *95*, 2508–2516. [3e] G. Dettlaff, E. Weiss, *J. Organomet. Chem.* **1976**, *108*, 213–223. [3f] L. J. Todd, J. P. Hickey, J. R. Wilkinson, J. C. Huffman, K. Folting, *J. Organomet. Chem.* **1976**, *112*, 167–176. [3g] F. R. Young III, D. H. O'Brien, R. C. Pettersen, R. A. Levenson, D. L. von Minden, *J. Organomet. Chem.* **1976**, *114*, 157–164. [3h] M. Casarin, D. Ajò, G. Granozzi, E. Tondello, S. Aime, *Inorg. Chem.* **1985**, *24*, 1241–1246. [3i] S. Aime, E. Occhiello, *J. Chem. Soc., Dalton Trans.* **1986**, 1863–1865. [3j] M. Tasi, A. K. Powell, H. Vahrenkamp, *Angew. Chem.* **1989**, *101*, 327–328; *Angew. Chem. Int. Ed. Engl.* **1989**, *28*, 318–319. [3k] R. Giordano, E. Sappa, D. Cauzzi, G. Predieri, A. Tiripicchio, M. T. Camellini, *J. Organomet. Chem.* **1991**, *412*, C14–C18. [3l] A. Marzotto, M. B. Cingi, A. Ciccarese, D. A. Clemente, *Acta Crystallogr., Sect. C* **1991**, *47*, 96–99. [3m] D. Seyferth, C. M. Archer, J. C. Dewan, *Organometallics* **1991**, *10*, 3759–3763. [3n] S. A. R. Knox, B. R. Lloyd, D. A. V. Morton, A. G. Orpen, M. L. Turner, G. Hogarth, *Polyhedron* **1995**, *14*, 2723–2743. [3o] R. Giordano, E. Sappa, D. Cauzzi, G. Predieri, A. Tiripicchio, *J. Organomet. Chem.* **1996**, *511*, 263–271. [3p] D. Osella, G. Dutto, C. Nervi, M. J. McGlinchey, A. Vessières, G. Jaouen, *J. Organomet. Chem.* **1997**, *533*, 97–102. [3q] R. Calderón, H. Vahrenkamp, *J. Organomet. Chem.* **1998**, *555*, 113–118. [3r] M. Barrow, N. L. Cromhout, D. Cunningham, A. R. Manning, P. McArdle, *J. Organomet. Chem.* **2000**, *612*, 61–68.
- [4] For examples of hydroxy ferrole complexes, see: [4a] A. A. Hock, O. S. Mills, *Proc. Chem. Soc. London* **1958**, 233–234. [4b] A. A. Hock, O. S. Mills, *Acta Crystallogr.* **1961**, *14*, 139–148. [4c] S. Aime, L. Milone, E. Sappa, A. Tiripicchio, A. M. M. Lanfredi, *J. Chem. Soc., Dalton Trans.* **1979**, 1664–1670. [4d] M. Periasamy, A. Mukkanti, D. S. Raj, *Organometallics* **2004**, *23*, 619–621.
- [5] [5a] M. A. Bennett, P. B. Donaldson, *Inorg. Chem.* **1978**, *17*, 1995–2000. [5b] S. J. Tyler, J. M. Burlitch, *J. Organomet. Chem.* **1989**, *361*, 231–247. [5c] I. Moldes, T. Papworth, J. Ros, A. Alvarez-Larena, J. F. Piniella, *J. Organomet. Chem.* **1995**, *489*, C65–C67. [5d] T. Henkel, A. Klauk, K. Seppelt, *J. Organomet. Chem.* **1995**, *501*, 1–6. [5e] R. J. Baxter, G. R. Knox, P. L. Pauson, M. D. Spicer, *Organometallics* **1999**, *18*, 197–205. [5f] H. Lang, G. Rheinwald, U. Lay, L. Zsolnai, G. Huttner, *J. Organomet. Chem.* **2001**, *634*, 74–82.
- [6] [6a] C. T. Sears Jr., F. G. A. Stone, *J. Organomet. Chem.* **1968**, *11*, 644–646. [6b] S. Aime, A. J. Deeming, *J. Chem. Soc., Dalton Trans.* **1981**, 828–832. [6c] A. Astier, J.-C. Daran, Y. Jeannin, C. Rigault, *J. Organomet. Chem.* **1983**, *241*, 53–68. [6d] M. I. Bruce, J. G. Matison, B. W. Skelton, A. H. White, *J. Organomet. Chem.* **1983**, *251*, 249–260. [6e] A. A. Koridze, A. I. Yanovsky, Y. T. Struchkov, *J. Organomet. Chem.* **1992**, *1*, 277–284. [6f] M. I. Bruce, N. N. Zaitseva, B. W. Skelton, A. H. White, *Inorg. Chim. Acta* **1996**, *250*, 129–138. [6g] S. P. Tunik, E. V. Grachova, V. R. Denisov, G. L. Starova, A. B. Nikol'skii, F. M. Dolgushin, A. I. Yanovsky, Y. T. Struchkov, *J. Organomet. Chem.* **1997**, *536*–537, 339–343. [6h] M. I. Bruce, B. W. Skelton, A. H. White, N. N. Zaitseva, *J. Organomet. Chem.* **1998**, *558*, 197–207. [6i] P. J. Low, G. D. Enright, A. J. Carty, *J. Organomet. Chem.* **1998**, *565*, 279–282. [6j] P. J. Low, K. A. Udachin, G. D. Enright, A. J. Carty, *J. Organomet. Chem.* **1999**, *578*, 103–114.
- [7] For other routes, see: [7a] I. Noda, H. Yasuda, A. Nakamura, *J. Organomet. Chem.* **1983**, *250*, 447–466. [7b] I. Noda, H. Yasuda, A. Nakamura, *Organometallics* **1983**, *2*, 1207–1214. [7c] H. Otori, H. Suzuki, Y. Moro-oka, *Organometallics* **1989**, *8*, 1576–1578. [7d] W. Krone-Schmidt, W. J. Sieber, N. M. Boag, C. B. Knobler, H. D. Kesz, *J. Organomet. Chem.* **1990**, *394*, 433–454. [7e] B. K. Campion, R. H. Heyn, T. D. Tilley, *Organometallics* **1990**, *9*, 1106–1112. [7f] X. D. He, B. Chaudret, F. Dahan, Y.-S. Huang, *Organometallics* **1991**, *10*, 970–979. [7g] L. A. Brady, A. F. Dyke, S. E. Garner, S. A. R. Knox, A. Irving, S. M. Nicholls, A. G. Orpen, *J. Chem. Soc., Dalton Trans.* **1993**, 487–488. [7h] M. Nishio, H. Matsuzaka, Y. Mizobe, T. Tanase, M. Hidai, *Organometallics* **1994**, *13*, 4214–4226. [7i] J. A. Cabeza, I. del Río, F. Grepioni, M. Mor-

- eno, V. Riera, M. Suárez, *Organometallics* **2001**, *20*, 4190–4197.
- [8] [8a] Y. Yamamoto, H. Kitahara, R. Ogawa, H. Kawaguchi, K. Tatsumi, K. Itoh, *J. Am. Chem. Soc.* **2000**, *122*, 4310–4319. [8b] Y. Yamamoto, R. Ogawa, K. Itoh, *J. Am. Chem. Soc.* **2001**, *123*, 6189–6190. [8c] Y. Yamamoto, S. Okuda, K. Itoh, *Chem. Commun.* **2001**, 1102–1103. [8d] Y. Yamamoto, H. Takagishi, K. Itoh, *Org. Lett.* **2001**, *3*, 2117–2119. [8e] Y. Yamamoto, H. Takagishi, K. Itoh, *J. Am. Chem. Soc.* **2002**, *124*, 28–29. [8f] Y. Yamamoto, H. Takagishi, K. Itoh, *J. Am. Chem. Soc.* **2002**, *124*, 6844–6845. [8g] Y. Yamamoto, K. Hata, T. Arakawa, K. Itoh, *Chem. Commun.* **2003**, 1290–1291. [8h] Y. Yamamoto, T. Arakawa, R. Ogawa, K. Itoh, *J. Am. Chem. Soc.* **2003**, *125*, 12143–12160. [8i] Y. Yamamoto, J. Ishii, H. Mishiya, K. Itoh, *J. Am. Chem. Soc.* **2004**, *126*, 3712–3713. [8j] Y. Yamamoto, K. Kinpara, T. Saigoku, H. Nishiyama, K. Itoh, *Org. Biomol. Chem.* **2004**, *2*, 1287–1294.
- [9] For examples of synthesis of dinuclear metallacycle complexes from α,ω -diynes, see: [9a] G. Predieri, A. Tiripicchio, M. T. Camellini, M. Costa, E. Sappa, *J. Organomet. Chem.* **1992**, *423*, 129–139. [9b] E. Boroni, M. Costa, G. Predieri, E. Sappa, A. Tiripicchio, *J. Chem. Soc., Dalton Trans.* **1992**, 2585–2590. [9c] K. Onitsuka, K. Miyaji, T. Adachi, T. Yoshida, K. Sonogashira, *Chem. Lett.* **1994**, 2279–2282. [9d] R. D. Adams, W. Fu, B. Qu, *J. Cluster Sci.* **2000**, *11*, 55–65.
- [10] For examples of cyclotrimerization of diyne diesters, see: [10a] P. Bhatarah, E. H. Smith, *J. Chem. Soc., Chem. Commun.* **1991**, 277–278. [10b] P. Bhatarah, E. H. Smith, *J. Chem. Soc., Perkin Trans. 1* **1992**, 2163–2168. [10c] Y. Yamamoto, A. Nagata, K. Itoh, *Tetrahedron Lett.* **1999**, *40*, 5035–5038. [10d] Y. Yamamoto, A. Nagata, H. Nagata, Y. Ando, Y. Arikawa, K. Tatsumi, K. Itoh, *Chem. Eur. J.* **2003**, *9*, 2469–2483. [10e] A. Jeevanandam, R. P. Korivi, I. Huang, C.-H. Cheng, *Org. Lett.* **2002**, *4*, 807–810. [10f] M. Shanmugasundaram, M.-S. Wu, M. Jegamohan, C.-W. Huang, C.-H. Cheng, *J. Org. Chem.* **2002**, *67*, 7724–7729. [10g] H. Nishiyama, E. Niwa, T. Inoue, Y. Ishima, K. Aoki, *Organometallics* **2002**, *21*, 2572–2574.
- [11] A. F. Hill, in *Comprehensive Organometallic Chemistry II*, vol. 7 (Eds.: E. W. Abel, F. G. A. Stone, G. Wilkinson, D. F. Shriver, M. I. Bruce), Pergamon, Oxford, **1995**, p. 406.
- [12] Similar (cyclopentadienone)ruthenium complexes have been reported, see: [12a] M. I. Bruce, J. R. Knight, *J. Organomet. Chem.* **1968**, *12*, 411–413. [12b] Y. Blum, Y. Shvo, D. F. Chodosh, *Inorg. Chim. Acta* **1985**, *97*, L25–L26. Also, see: [12c] E. Rüba, K. Mereiter, K. M. Soldouzi, C. Gemel, R. Schmid, K. Kirchner, E. Bustelo, M. C. Puerta, P. Valerga, *Organometallics* **2000**, *19*, 5384–5391, and references cited therein. [12d] A. F. Hill, A. D. Rae, M. Schultz, A. C. Willis, *Organometallics* **2004**, *23*, 81–85.
- [13] [13a] O. S. Mills, G. Robinson, *Proc. Chem. Soc. London* **1964**, 187. [13b] J. Wessel, H. Hartl, K. Seppelt, *Chem. Ber.* **1986**, *119*, 453–463. [13c] G. Gervasio, E. Sappa, L. Markó, *J. Organomet. Chem.* **1993**, *444*, 203–209. [13d] R. J. Baxter, G. R. Knox, J. H. Moir, P. L. Pauson, M. D. Spicer, *Organometallics* **1999**, *18*, 206–214. [13e] F.-E. Hong, J.-Y. Wu, Y.-C. Huang, C.-K. Hung, H.-M. Gau, C.-C. Lin, *J. Organomet. Chem.* **1999**, *580*, 98–107.
- [14] [14a] L. H. Staal, L. H. Polm, K. Vrieze, F. Ploeger, C. H. Stam, *J. Organomet. Chem.* **1980**, *199*, C13–C16. [14b] K. A. Johnson, W. L. Gladfelter, *Organometallics* **1989**, *8*, 2866–2871. [14c] K. A. Johnson, W. L. Gladfelter, *J. Am. Chem. Soc.* **1991**, *113*, 5097–5099. [14d] K. A. Johnson, W. L. Gladfelter, *Organometallics* **1992**, *11*, 2534–2542. [14e] J. S. Field, R. J. Haines, J. Sundermeyer, S. F. Woollam, *J. Chem. Soc., Dalton Trans.* **1993**, 3749–3757Å.
- [15] G. M. Sheldrick, *SHELXTL 5.1*, Bruker AXS Inc., Madison, Wisconsin, **1997**.

Received February 14, 2004

Early View Article

Published Online June 24, 2004